Acta metall. Vol. 30, pp. 1883 to 1890, 1982
Printed in Great Britain.

0001-6160/82/101883-08$03.00/0

THE INFLUENCE OF AN INCREASING PARTICLE COORDINATION ON THE DENSIFICATION OF SPHERICAL POWDERS

E. ARZT
Engineering Department, Cambridge University, Cambridge, England

(*Received* 1 *May* 1982)

Abstract—The densification of spherical powders by cold compaction, hot-isostatic pressing and sintering can be described in terms of the shrinkage of the Voronoi cells associated with the initial packing of the powder particles. The shape of the average cell is determined by the radial distribution function of a 'random dense' packing of spheres. The advantage of this approach lies in its ability to explain quantitatively the continuous formation of new neighbours (increase in particle 'coordination'). Using simple constitutive relations for low temperature plasticity, diffusion, and power-law creep, the effects of an increasing coordination on densification by these mechanisms are assessed. The results show that in pressing operations, with negligible contribution from diffusion, densification becomes increasingly more difficult than would be expected on the basis of constant coordination; that in sintering, on the other hand, densification rates are underestimated by two-sphere models.

Résumé—On peut décrire la densification de poudres sphériques par compactage à froid, formage isostatique à chaud et frittage à partir du rétrécissement des cellules de Voronoi associées à la configuration initiale des particules de la poudre. La taille de la cellule moyenne est déterminée par la fonction de répartition radiale d'un empilement "aléatoire dense" de sphères. L'avantage de cette approche réside dans la possibilité d'expliquer quantitativement la formation continue de nouveaux voisins (augmentation de la "coordination" des particules). En utilisant des des relations de constitution simples pour la plasticité à basse température, la diffusion et le fluage selon une loi en puissance, nous avons vérifié les effets d'un accroissement de la coordination sur la densification par ces mécanismes. Nos résultats montrent qu'au cours du formage avec une contribution négligeable de la diffusion, la densification devient plus difficile qu'onne s'y attendrait sur la base d'une coordination constante; D'autre part, ils montrent également qu'au cours du fluage les vitesses de densification sont sous-estimées par les modèles à deux sphères.

Zusammenfassung—Die Verdichtung sphärischer Pulver durch Kaltpressung, isostatischer Warmpressung und Sintern kann mit der Schrumpfung von Voronoizellen, die mit der Anfangspackung der Pulverteilchen zusammenhängen, beschrieben werden. Die mittlere Zellform wird bestimmt durch die radiale Verteilungsfunktion einer 'zufällig-dichten' Packung von Kugeln. Der Vorteil dieser Näherung liegt darin, daß die kontinuierliche Bildung neuer Nachbarn (Anstieg der Teilchen-'Koordination') quantitative erklärt werden kann. Mit einfachen Grundgleichungen für die Niedertemperaturplastizität, die Diffusion und das Potenzgesetzkriechen werden die Effekte einer zunehmenden Koordination bei der Verdichtung abgeschätzt. Es zeigt sich, daß die Verdichtung ohne einen wichtigen Beitrag durch Diffusion immer schwieriger wird verglichen mit konstant bleibender Koordination. Andererseits werden beim Sintern die Verdichtungsgeschwindigkeiten im Zweikugelmodell unterschätzt.

1. INTRODUCTION

Most theories of the densification behaviour of powders subjected to high temperature (as in sintering) and/or pressure (as in hot and cold compaction) deduce the shrinkage from the linear densification between two spherical particles in a regular packing. This approach neglects the peculiarities arising from the fact that the particle structure is never regular and changes continually during densification. As the average particle distance decreases, the particles are squeezed together and form contact areas. During this process the average number of contacts per particle ("coordination number") increases steadily. This implies that in pressing operations the forces acting on the particle contacts diminish continuously, because the external pressure is shared among an increasing number of contacts. In sintering the opposite effect occurs: the densification rate is roughly proportional to the number of contacts per unit volume. In both cases the geometry of the particle packing may therefore influence the densification; to what extent remains to be seen.

Sphericity of particles is a convenient, and (in view of the increasing technological importance of spherical powders) realistic model assumption. The two-sphere approach has been criticized on the grounds that it fails to account for processes observed in model experiments, particularly particle rearrangement and pore opening [1]. It has recently been shown [2], however, that numerical simulations of the shrinkage behaviour of three-dimensional particle

structures give results close to the two-sphere model. The remaining slight discrepancy has been explained by invoking the formation of new contacts. It can therefore be expected that a quantitative treatment of contact formation could fill an important gap in our understanding of powder densification.

This paper describes how the change in coordination can be accounted for quantitatively by assuming the particle structure to be a 'random dense' sphere packing with a simple radial distribution function. We derive analytic expressions for contact number and contact area as functions of relative density. On this basis, the influence of the coordination number on the processes of hot and cold compaction and on sintering will be discussed. The symbols used are listed in the Table.

Table of symbols

$G(r)$	cumulative radial distribution function (RDF) of the particle packing
C	slope of linearized $G(r)$ of a random dense packing (see Fig. 1)
R	initial particle radius (taken as 1)
Z	average coordination number
Z_0	average coordination number at start of densification
a	average contact area (measured in units of R^2)
D	relative density of compact
D_0	relative density at start of densification
R'	fictitious sphere radius after densification (see Fig. 3)
R'', R''_{cor}	particle radius after material redistribution (see Fig. 3)
p	external pressure in cold compaction and hot-isostatic pressing
P_{eff}	"effective pressure" (pressure acting on an average contact face)
$\dot{\varepsilon}_0, \sigma_0$	power-law creep material parameters (see equation 22)

2. THE POWDER AS A RANDOM PACKING

The initial densification of a powder may be due to the relative motion of particles by sliding. In spherical powders this process is confined to the very beginning of densification, even if a pressure is applied [3]. During pressureless sintering, rearrangement of particles may take place owing to the presence of asymmetrical necks [1]. In three-dimensional packings with usual fill densities, however, this movement will be strongly impeded by neighbouring particles. Any kind of rearrangement could of course affect the evolution of contact number and contact area, but we will neglect these mechanisms in the present treatment.

In a packing without sliding, densification can be brought about only by centre-to-centre approach of particles. During shrinkage new particle pairs will be brought close enough to form additional contacts. A study of the geometrical changes during cold compaction of a spherical powder [3] has shown this to be a continuous process: the coordination number, about 7.3 in the original packing, increases steadily (and faster than the density) as densification proceeds. A regular lattice-type packing cannot account for this behaviour. Therefore the change in coordination is neglected in current two-particle theories.

A continuous increase in coordination can be modelled by assuming a 'random' particle structure with a continuous distribution of centre-to-centre distances. Whether a particular sphere of the packing is likely to form a new contact at a certain stage of densification depends upon the distribution of particles in its immediate vicinity. The arrangement of near-neighbours of a representative reference sphere can be characterized by the distribution of centre distances ('radial density function', RDF), or—more conveniently in the present context—by its integral, the cumulative radial distribution function, $G(r)$. $G(r)$ states the number of particle centres within a fictitious sphere of radius r around the reference sphere. Scott [4] and Mason [5] have published RDFs of a 'random dense' packing (Fig. 1). Their results show that, in the narrow range of interest ($r < 2.8\,R$) $G(r)$ can be approximated by

$$G(r) = 0 \qquad \text{for} \quad r < 2R$$
$$G(r) = Z_0 + C\left(\frac{r}{2R} - 1\right) \qquad r \geq 2R \tag{1}$$

where $Z_0 = 7.3$ is the average coordination number of the packing, $C = 15.5$ is the slope of the RDF, and R the particle radius. This approximation neglects a slight curvature of $G(r)$ in the range $2R < r < 2.1\,R$, which must be of little importance, as the linearly extrapolated value ($Z_0 = 7.3$) coincides with the average coordination number of a sieved spherical powder [3]. Also, the relative density of a random dense packing ($D_0 = 0.64$) corresponds closely to the tap density of the same powder. We therefore feel justified to regard the random dense packing with a linearized $G(r)$ as a realistic model for the geometric structure of a spherical monosize powder.

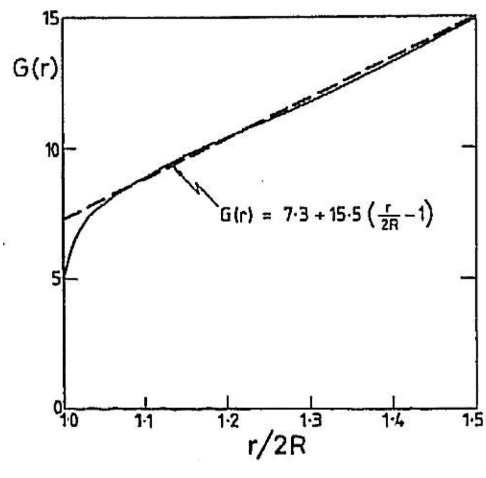

Fig. 1. The cumulative radial distribution function (RDF) of a random dense packing, obtained by Mason [5] from data by Scott [4]. Broken line: linear approximation used in calculations.

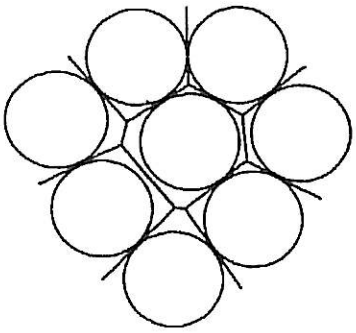

Fig. 2. Two-dimensional schematic of the division of the powder bed into Voronoi cells. The non-contacting neighbours sharing a cell wall will form contacts as densification proceeds.

3. DENSIFICATION OF A RANDOM DENSE PACKING

During densification each particle changes its shape by forming contact areas with its neighbours until, at full density, the sphere packing has been converted into a space-filling stack of irregular polyhedra. If, as it is assumed here, the densification has been homogeneous, then these polyhedra are identical in shape with the Voronoi polyhedra† of the original packing (Fig. 2). Densification can be visualized as the shrinkage of these polyhedra; the deformation of the particles can be regarded as imposed by the walls of the shrinking cells.

At any given moment the coordination number is equal to the number of Voronoi faces in contact with the particle surface. The average contact area can be calculated from the amount of flattening the reference particle has undergone.

Now we combine the concepts of the RDF and the Voronoi polyhedra. The distribution of the distances from the faces to the centre of an average Voronoi polyhedron is identical with the RDF, equation 1 (apart from a factor 2: the number of initial neighbours, for instance, is equal to the number of faces at the distance of *one* particle radius). Suppose that during densification, the centres and the polyhedra remain fixed, so that the RDF stays invariant. Densification is modelled by the concentric growth of the spherical particles. The new (fictitious) particle radius R' is obtained by noting that in our model system, the apparent volume of N particles is independent of density

$$N\frac{4\pi R^3}{3D_0} = N\frac{4\pi R'^3}{3D} \qquad (2)$$

† The Voronoi polyhedron [6] or Dirichlet cell [7] of a particle in a packing is the set of all points in space which are closer to its centre than to any other particle centre. The boundaries of this polyhedron are obtained by placing perpendicular bisecting planes on all centre-to-centr3 connections. In the present context it is important to note that the faces of the Voronoi polyhedra contain all the contact areas.

$D_0 = 0.64$ is the relative fill density of a random dense packing, D the current relative density, R the original particle radius, which we take to be 1. Hence

$$R'(D) = \left(\frac{D}{D_0}\right)^{1/3}. \qquad (3)$$

After the spheres have grown to this new radius, some of them overlap, i.e. they reach into neighbouring polyhedra at cell faces whose distance from the centre $r < R'$ (Fig. 3 II). According to equation 1, the number of these overlaps is

$$Z(D) = G[2R'(D)] = Z_0 + C(R' - 1). \qquad (4)$$

This simple equation describes the increase in coordination due to the reduction of particle distances. Since new contacts may also form as a result of the change in contact geometry (especially at later stages), equation 4 represents a lower bound for the average coordination number. The total sphere volume cut off by the Voronoi faces ('excess volume', shaded in Fig. 3 II) can be determined by integration over initial and newly-formed contacts (Appendix)

$$V_{ex} = \frac{\pi}{3}Z_0(R' - 1)^2(2R' + 1) + \frac{C\pi}{12}(R' - 1)^3(3R' + 1). \qquad (5)$$

This excess material is in reality transported away from the contact zone by plastic flow, diffusion or creep. In terms of the model, the shape accomodation

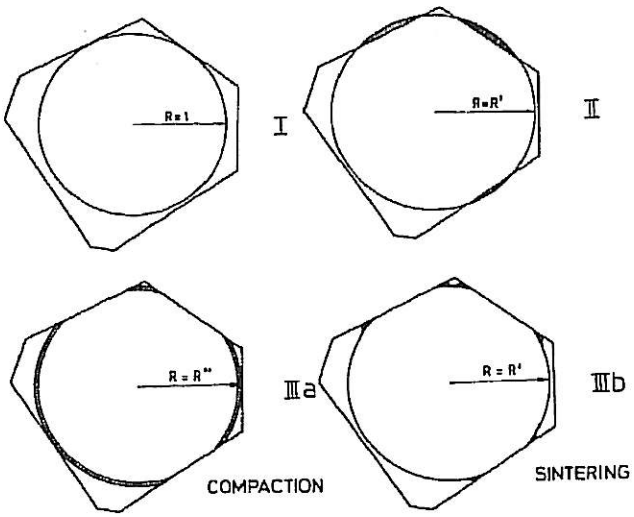

Fig. 3. The geometry of the model: starting from an average particle, with an average Voronoi cell (I), densification is modelled as concentric growth of the particle, beyond the stationary walls of its cell (new particle radius R') (II). The excess volume outside the polyhedron (shaded) is redistributed either (a) evenly across the free surface of the sphere; this produces a truncated sphere of radius R'' ('compaction' case, IIIa), or (b) near the contact region, forming necks ('sintering' case, IIIb). Then the average area of contact between the particle and the cell walls are calculated in each case. The coordination numbers are given by the RDF of the packing: $G(2R'')$ and $G(2R')$, respectively. An iteration step replaces R'' with R''_{cor} (see text).

is achieved by redistributing the excess material within its own Voronoi cell. Depending on the mechanism, it will stay more or less in the vicinity of the contacts. Since it is difficult to describe the geometry of the contacts accurately by analytical expressions, we will consider two tractable limiting cases:

(i) *Long-range redistribution:* the excess material is deposited evenly across that portion of the sphere surface which has remained within the cell (Fig. 3, IIIa). This assumption will lead to a lower bound for the size of the contacts and an upper bound for the coordination number. The assumed contact geometry resembles that after pressure densification, with little or no contribution from diffusion.

(ii) *Short-range redistribution:* the excess material stays in the vicinity of the contact and is used to form 'necks' between the particles (Fig. 3, IIIb). In this case an upper bound for the contact areas and a lower bound for the coordination numbers will result. The formation of a distinct neck is characteristic of densification by diffusion, as in pressureless sintering.

3.1 *Long-range redistribution (approximation for pressure densification)*

If the excess material V_{ex} is distributed evenly across the free spherical surface of area S, truncated spheres of a new radius R'' are created. Conservation of volume requires

$$\frac{4\pi}{3}(R''^3 - R'^3)\frac{S}{4\pi R'^2} \simeq (R'' - R')S = V_{ex}. \quad (6)$$

S is the surface of the sphere of radius R', reduced by the areas of contact. At the beginning of redistribution (Appendix)

$$S = 4\pi R'^2 - 2Z_0\pi R'(R' - 1) - C\pi R'(R' - 1)^2. \quad (7)$$

Combining equations (5), (6) and (7), R'' can be determined

$$R'' = R' + \frac{4Z_0(R' - 1)^2(2R' + 1) + C(R' - 1)^3(3R' + 1)}{12R'[4R' - 2Z_0(R' - 1) - C(R' - 1)^2]}. \quad (8)$$

The average contact area is obtained by averaging over all existing contacts: Z_0 contacts of maximum size (initial contacts) and some progressively smaller ones (newly-formed) (Appendix). This average area, in units of R^2, is

$$a = \frac{\pi}{3ZR'^2}[3(R''^2 - 1)Z_0 + R''^2(2R'' - 3)C + C]. \quad (9)$$

So far we have neglected the fact that sphere growth and material redistribution occur simultaneously; that additional excess material is created at new contacts; and that the free surface S available for material deposition decreases continuously. These are second-order effects which will exert much influence on the evolution of contact numbers only at high densities. Incorporating them in our theory would require an iterative procedure. Analytical tractability can be preserved if we perform one single iteration step which leads to a reasonable approximation for a corrected R'' (Appendix)

$$R''_{cor} = R' + \frac{4Z_0(R' - 1)^2(2R' + 1) + C(R'' - 1)^3(3R'' + 1)}{12[4R'^2 - 2Z_0R'(R' - 1) - CR''(R'' - 1)^2]} \quad (10)$$

where R' is obtained from equation 3, and R'' from equation (8).

The coordination number is equal to the value of $G(r)$ at $r = 2R''_{cor}$

$$Z(D) = G(2R''_{cor}) = Z_0 + C(R''_{cor} - 1). \quad (11)$$

While equation (4) took account of the increase in coordination only due to reduced particle distances, equation (11) allows for an additional change resulting from the contact deformation. Note that we have not inserted R''_{cor} in equation (9); at the stage when this correction becomes significant, the growth of contact areas is impeded by the mutual impingement of neighbouring contacts (as discussed by Fischmeister and Arzt [8]). From then on the model is no longer strictly valid.

3.2 *Short-range redistribution (approximation for pressureless sintering)*

In this case, it is assumed that the excess material at each cell face forms a neck between the particle and its neighbour at that face. We neglect any other contributions to neck growth, e.g. diffusion from surface sources, evaporation—condensation, etc. The neck surface is usually modelled as a torus surface; the contact area is then given by an implicit function [9] of the relative centre approach h/R. For this relationship, we will use the following approximation

$$a = 11\,h/R. \quad (12)$$

Translating into the present model geometry, we get for the contact area at a cell face at a distance r from the cell centre

$$a(r) = 11\left(1 - \frac{r}{R'}\right). \quad (13)$$

Hence, the average contact area is (Appendix)

$$a = \frac{11}{ZR'}\left[Z_0(R' - 1) + \frac{C}{2}(R' - 1)^2\right]. \quad (14)$$

It has been assumed that the material redistribution affects only the immediate neighbourhood of the contacts and not the parts of the sphere surfaces between

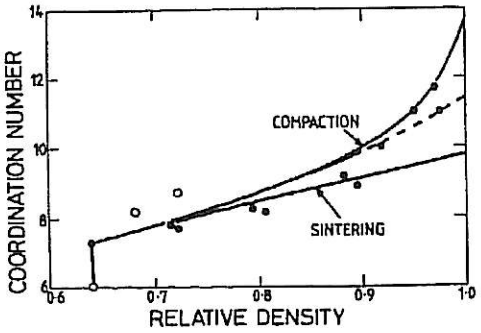

Fig. 4. Average coordination number vs relative density. Upper curve is $G[2R''_{cor}(D)]$, centre curve $G[2R''(D)]$, and lower curve $G[2R'(D)]$. Solid circles are data from compacted bronze powder [3], open circles results of computer simulations [2].

contacts where formation of new contacts is most likely. The increase in coordination must therefore be described by equation (4), at least until contact faces start to impinge on the particle surfaces. According to the model, this happens at a relative density of about 90%. From then on material redistribution will contribute to the formation of new contacts in a similar way as in long-range redistribution. The coordination number will approach the curve corresponding to the pressing limit, while the exact path taken will depend on the densifying mechanism.

The results of the calculations are shown in Figs 4 and 5. Coordination numbers according to equations (4) and (11) are compared with values measured on pressed specimens. At first, the points conform rather to the lower curve (sintering limit), which is a reflection of the fact that also in pressing the contact material tends to stay at first in the vicinity of the contact. At higher densities the agreement with the upper curve is good, and the final coordination, predicted as 13.69, coincides with the results of numerous experimental and theoretical studies [10, 11, 12]. Also included in Fig. 4 are the coordination numbers obtained from computer simulations by Ross *et al.* [2]. These data, being based on perfectly monosize spheres, reflect the initial curvature of the RDF, which we have ignored in equation 1. After elimination of about 2% porosity the values show the same slope as predicted, but are generally somewhat higher.

For contact areas, data from both sintered and compacted specimens, and from model experiments with particle pairs, are available (Fig. 5). They show that there is a clear, predictable distinction in the evolution of contact area depending on whether contact growth is predominantly by diffusion or by plasticity. The two 'sintering' curves show that towards full density the choice of the coordination number, Z, in equation (14) becomes important. If, because of the impingement mentioned above, we use Z for the pressing limit, equation (11), then the centre curve in Fig. 5 is obtained. This curve makes sense, because at full density it intersects the 'compaction' curve at an area value which corresponds to the average face area of a tetrakaidekahedron. If, on the other hand, Z from equation (4) is used, then the upper curve results, predicting unrealistically large contact areas at high densities.

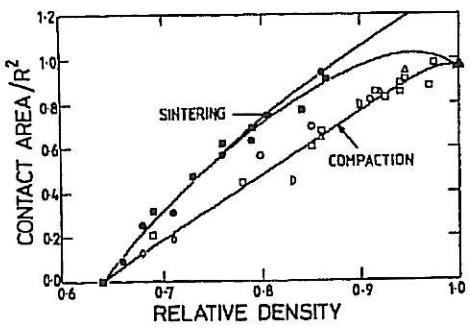

Fig. 5. Average contact area vs relative density. Centre curve uses Z for pressing limit (see text). Experimental data: open symbols, compacted powder (○ Copper [19], ◇ Lead [18], Zinc [19], △ Aluminium [19], □ Bronze [3]); solid symbols, sintered powder (● Copper [9], ■ Glass [9]). ▲ average contact area in a stack of equal tetrakaidekahedra.

4. APPLICATIONS

The foregoing considerations have shown how the assumption of a random packing allows both the growth of contact areas and the increase in coordination to be described. Being purely geometric they apply regardless of the particular mechanism by which a centre-approach is achieved. For the application of the model to actual densification processes, these results have to be combined with the appropriate constitutive equations. This will be done for cold compaction, hot pressing and pressureless sintering.

For our purposes, the following approximate expressions (obtained for $Z_0 = 7.3$, $C = 15.5$ and $D_0 = 0.64$) are useful. The coordination number in the sintering limit, equation (4), is

$$Z = Z_0 + C\left[\frac{D - D_0}{3D_0} - \left(\frac{D - D_0}{3D_0}\right)^2 + - \cdots\right]. \quad (15)$$

Neglecting all terms in this series except the first one gives a maximum deviation from equation (4) of 4%; including the second term improves accuracy to 1%.

The coordination number in the pressing limit [equation (11)] is

$$Z = Z_0 + 9.5(D - D_0) \text{ for } D < 0.85 \quad (16)$$

$$Z = Z_0 + 2 + 9.5(D - 0.85) + 881(D - 0.85)^3. \quad \text{for } D > 0.85$$

with a maximum error of 2%.

The average contact area in the sintering limit (equation 14) is

$$a = 5.5\,(D - D_0)\,[1 - (D - D_0)] \pm 4\%. \quad (17)$$

The average contact area in the pressing limit (equation 9) is

$$a = 3\,(D - D_0) \pm 8\% \quad (18)$$

(maximum deviation in the range $0.7 < D < 0.95$: 4%).

4.1 *Cold compaction*

When a pressure is applied to a powder at room temperature, the densification is by (low-temperature) *plastic flow* at the particle contacts. Locally the following yield criterion must be satisfied (indentation solution) [13]

$$\frac{f}{a} = 3\sigma_f \quad (19)$$

where f/a is the 'effective pressure' which acts on an average particle contact, a the contact area, and σ_f the flow stress of the material.

For isostatic compression of a random sphere packing the correlation between local contact force f and the external pressure p is [14]

$$f = \frac{4\pi}{ZD}\,p \quad (20)$$

(for die compression, where pressure is dissipated by die-wall friction, p would have to be replaced by the local pressure). The effective pressure is then

$$P_{\text{eff}} = \frac{f}{a} = \frac{4\pi p}{a(D)Z(D)D}. \quad (21)$$

By combining equations (19) and (21) and allowing for a density-dependent flow stress (because of work hardening), a complete theory of isostatic cold compaction has been developed, which is in good agreement with experimental results [8].

It is important to note that in this model for cold compaction only the product $a \cdot Z$ (i.e. the total contact area) enters the equations. In Fig. 6 the correction factor by which the effective pressure is changed (with regard to calculations assuming constant coordination) is plotted as a function of relative density (curve marked 'cold compaction').

4.2 *Hot isostatic pressing (HIP)*

In hot pressing, the instantaneous densification is again due to rate-independent plasticity. When yielding stops, the contact regions continue to deform by power-law creep and/or diffusional flow. Because process cycle times are of the order of hours, these time-dependent mechanisms usually supply most of the densification.

If the powder material exhibits power-law creep according to

$$\dot{\epsilon} = \dot{\epsilon}_0 \left(\frac{\sigma}{\sigma_0}\right)^n \quad (22)$$

(where $\dot{\epsilon}_0$ and σ_0 are material properties) then the densification rate caused by *power-law creep* alone is [15]

$$\frac{dD}{dt} = 5.3(D^2 D_0)^{1/3}\dot{\epsilon}_0 \sqrt{\frac{a}{\pi}} \left(\frac{P_{\text{eff}}}{3\sigma_0}\right)^n \quad (23)$$

where P_{eff} is given by equation (21) (we ignore surface tension as a driving force because it is usually insignificant in HIP).

From equations (23) and (21) it follows that

$$\frac{dD}{dt} \propto \frac{\sqrt{a}}{(aZ)^n}. \quad (24)$$

Figure 6 shows the error introduced by neglecting the increase in coordination for a material with $n = 3$ (curve marked 'HIP-Creep $n = 3$').

Diffusional creep supplies a densification rate which can be obtained by equating the rate of volume deposition by diffusion [16, 17] to the rate of excess volume removal (the derivative of equation (5) with respect to time). The result is [15]

$$\frac{dD}{dt} = \frac{12D^2}{D_0}\,\frac{(\delta D_b + \rho D_v)\Omega}{kTR^3}\,ZP_{\text{eff}} \times \frac{1}{Z_0(R'^2 - 1) + \frac{C}{4}(R'^2 - 1)^2} \quad (25)$$

where D_b and D_v are the grain boundary and lattice diffusivities and ρ the neck curvature (and the absolute

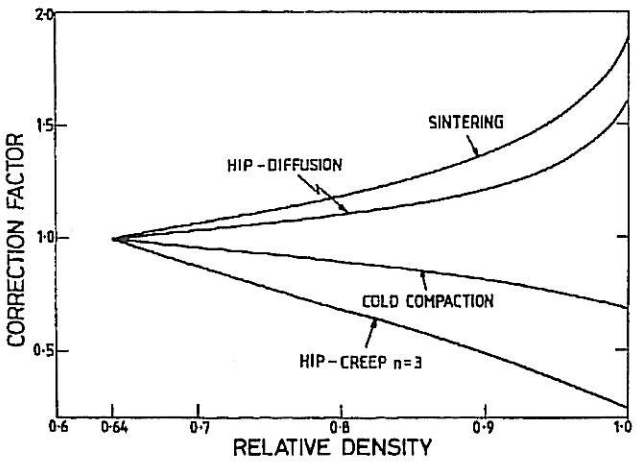

Fig. 6. Ratios (present calculations/calculations assuming constant coordination). In 'cold compaction', effective pressures are compared (equation 21); in all other cases, approximated densification rates (equations 28, 26, 24).

value of R enters because it determines the diffusion distances). In this case

$$\frac{dD}{dt} \propto ZP_{\text{eff}} \propto \frac{1}{a}. \quad (26)$$

The rate of densification is inversely proportional to the *average contact area*. Therefore, one would expect that a larger number of small contacts will lead to faster densification than a smaller number of larger ones, $a \cdot Z$ being equal. This is again illustrated in Fig. 6, where the error made by assuming a constant coordination is plotted as a function of relative density (curve 'HIP-Diffusion').

Based on these and similar equations, mechanism maps can be constructed which predict the extent of densification and identify the dominant mechanism during hot-isostatic pressing [15].

4.3 *Pressureless sintering*

In pressureless sintering driving forces for densification appear only at particle contacts (unlike pressure densification, where the driving force is supplied by the external pressure and is consumed by the contacts). New contacts therefore introduce additional driving forces; and a stronger dependence of densification rates on coordination is expected.

An expression for the densification rate due to diffusion may be obtained from equation 25 by identifying P_{eff} with the capillary stress (which is insensitive to changes in Z)

$$\frac{dD}{dt} = \frac{12D^2}{D_0} \frac{(\delta D_b + \rho D_v)\Omega Z}{kTR^3} \gamma \left(\frac{1}{\rho} - \frac{1}{x}\right) \times \frac{1}{Z_0(R'^2 - 1) + \frac{C}{4}(R'^2 - 1)^2} \quad (27)$$

where γ is the surface energy and $x = \sqrt{a/\pi}$ the average contact radius. Hence, densification is determined roughly by the number of contacts per volume of compact

$$\frac{dD}{dt} \propto \frac{ZD}{R^3}. \quad (28)$$

The increase in coordination should therefore be directly reflected in the densification rate. From Fig. 6 ('sintering' curve) it is clear that pressureless sintering is most sensitive to changes in coordination.

5. DISCUSSION AND CONCLUSION

It has been shown that the assumption of a random dense packing as a model for the initial particle structure allows a more precise prediction of the particle geometry during densification by plastic flow and creep. All geometric elements have been supplied for modelling the usual powder metallurgical production route (comprising cold compaction and subsequent sintering), and hot-isostatic pressing.

Particle rearrangement and the possibility of inhomogeneous densification have been ignored in the present treatment, because these mechanisms are difficult to model. The theory does not claim to cover 'low-coordination' arrays in the sense of Ross *et al.* [3]. The calculations show that the increase in coordination is slow at first: this justifies the assumption of constant coordination for 'stage 1' models. A dramatic change in coordination occurs only at densities above about 90%, when contacts have impinged [8]. At that stage the present model, which assumes uninhibited growth of contact areas, is no longer strictly valid. The iteration step introduced in equation (11) happens to lead to a reasonable final coordination, however, and the contact area at full density corresponds closely to the average contact area in a stacking of equal tetrakaidekahedra. These observations, and the agreement with experimental data (Figs 4 and 5), support the model strongly even at high densities, at which most theories resort to representing the pores simply by spherical cavities.

The information about both the average contact area and the coordination number (and not only the total contact area) can be important for calculating the effective pressure and densification rates (Fig. 6). In cold pressing, new contacts reduce the average contact force and compaction becomes increasingly more difficult than would be expected on the basis of constant coordination. This 'geometric hardening' effect is even more pronounced when the densification occurs mainly by power-law creep of the powder material (as in hot-isostatic pressing, in certain temperature-pressure regimes [15]): in a material with the power-law exponent $n = 3$, for instance, the rate of densification may drop by a factor of up to three only as a result of the increase in coordination (Fig. 6).

When diffusion is the dominant densifying mechanism (as in pressureless sintering, or hot-isostatic pressing), new contacts, owing to their higher neck curvature, will tend to speed up densification, or rather, slow down the inevitable decrease of sintering rates due to the continuous reduction of the capillary stress at the growing contacts. Therefore, densification rates are always higher than for a particle packing with constant coordination (Fig. 6). As expected, the 'accelerating' effect is most prominent in pressureless sintering.

One limitation of the present model is quite obvious: the interactions of different neighbours of one sphere are not taken into account explicitly. New contacts, even if they tend to bring about faster centre approach, will always be constrained by neighbouring particles. This leads to a complicated stress state. Overall densification will not be determined by the size of the largest contacts, nor by the smallest ones. This model is a compromise: it likens shrinkage of the powder bed to the densification experienced by a representative particle with the average number of

average-size contacts, surrounded by an "average" Voronoi cell. We suggest this approach, which is still amenable to an analytical treatment, as a step towards a more realistic description of powder densification.

Acknowledgements—I would like to thank Professors H. Fischmeister and M. F. Ashby for numerous discussions. This work was supported, in its earlier stages, by the Austrian Fonds zur Förderung der wissenchaftlichen Forschung and, subsequently, by the S.E.R.C. (U.K.).

REFERENCES

1. G. Petzow and H. E. Exner, *Z. Metallk.* **67**, 611 (1976).
2. J. W. Ross, W. A. Miller and G. C. Weatherly, *Acta metall.* **30**, 203 (1982).
3. H. F. Fischmeister, E. Arzt and L. R. Olsson, *Powder Metall.* **21**, 179 (1978).
4. G. D. Scott, *Nature* **194**, 956 (1962).
5. G. Mason, *Nature* **217**, 733 (1968).
6. G. F. Voronoi, *J. reine angew. Math.* **134**, 198 (1908).
7. G. L. Dirichlet, *J. reine angew. Math.* **40**, 216 (1850).
8. H. F. Fischmeister and E. Arzt, *Powder Metall.* To be published.
9. H. E. Exner, *Rev. Powder Metall. Phys. Ceram.* **1**, 7 (1979).
10. J. W. Marvin, *J. Botany* **26**, 280 (1939).
11. H. S. M. Coxeter, *Illinois J. Math.* **2**, 746 (1958).
12. J. D. Bernal, *Nature* **183**, 141 (1959).
13. R. Hill, '*The Mathematical Theory of Plasticity*' p. 254. Clarendon Press, Oxford (1960).
14. O. Molerus, *Powder Technol.* **12**, 259 (1975).
15. E. Arzt, M. F. Ashby and K. E. Easterling, *Metall. Trans.* To be published.
16. D. L. Johnson, *J. appl. Phys.* **40**, 192 (1969).
17. D. S. Wilkinson, Ph.D. Thesis, Univ. of Cambridge (1977).
18. A. K. Kakar and A. C. D. Chaklader, *J. appl. Phys.* **38**, 3223 (1967).
19. P. J. James, *Powder Metall.* **20**, 199 (1977).

APPENDIX

Calculations

The excess volume created at an initial contact is the volume of a spherical cap of height $(R' - 1)$

$$V_0 = \frac{\pi}{3}(R' - 1)^2(2R' + 1). \tag{A1}$$

At a polyhedron face at a distance r from the cell centre

$$V_1(r) = \frac{\pi}{3}(R' - r)^2(2R' + r). \tag{A2}$$

Remembering that according to equation (1) an infinitesimal increase in contact number is $dN = C\,dr$, the total excess volume is

$$V_{ex} = V_0 \cdot Z_0 + C\int_{r=1}^{R'} V_1(r)\,dr \tag{A3}$$

from which follows equation (5).

The portion of the sphere surface available for material deposition is the total sphere surface minus old and new contact areas. One initial contact occupies an area

$$S_0 = 2\pi R'(R' - 1) \tag{A4}$$

a new contact

$$S_1(r) = 2\pi R'(R' - r). \tag{A5}$$

The free surface is then

$$S = 4\pi R'^2 - S_0 \cdot Z_0 - C\int_{r=1}^{R'} S_1(r)\,dr \tag{A6}$$

which, evaluated, yields equation (7).

The average contact area is a function of R'' (equation (9)). For initial contacts

$$a_0 = (R''^2 - 1)\pi. \tag{A7}$$

Newly-formed contacts have smaller contact areas

$$a_1(r) = (R''^2 - r^2)\pi. \tag{A8}$$

The average contact area (equation (9)) is then obtained from

$$a = \frac{1}{ZR'^2}\left[a_0 Z_0 + C\int_{r=1}^{R''} a_1(r)\,dr\right] \tag{A9}$$

(where the factor $1/R'^2$ normalizes the result to the original particle radius $R = 1$).

Having so far neglected all contacts that are formed during material redistribution, we can improve the result by treating R'' (from equation (8)) as a new R'. Then the additional excess volume is

$$V_2(r) = \frac{\pi}{3}(R'' - r)^2(2R'' + r) - V_1(r). \tag{A10}$$

The additional surface area occupied is

$$S_2(r) = 2\pi R''(R'' - r) - S_1(r). \tag{A11}$$

From the balance of volumes

$$(R''_{cor} - R')\left(S - C\int_{r=1}^{R'} S_2(r)\,dr\right) = V_{ex} + C\int_{r=1}^{R'} V_2(r)\,dr \tag{A12}$$

equation (10) follows immediately.

The average contact area for the case of short-range redistribution is obtained by integrating equation (13) as in equation (A9)

$$a = \frac{11}{ZR'}\left[Z_0(R' - 1) + C\int_{r=1}^{R'}(R' - r)\,dr\right] \tag{A13}$$

$$= \frac{11}{ZR'}\left[Z_0(R' - 1) + \frac{C}{2}(R' - 1)^2\right]. \quad \text{(A14)} = (14)$$